Available online at www.sciencedirect.com
SCIENCE DIRECT®
Journal of Photochemistry and Photobiology A: Chemistry 174 (2005) 253–260
Journal of Photochemistry and Photobiology A:Chemistry
www.elsevier.com/locate/jphotochem

Enhanced photodegradation of diisopropyl methyl phosphonate by the "Adsorb & Shuttle" approach

Yelena Sagatelian, Dovrat Sharabi, Yaron Paz *

Department of Chemical Engineering, The Grand Water Research Institute and The Institute of Catalysis, Technion, Haifa 32000, Israel

Received 6 December 2004; received in revised form 24 February 2005; accepted 16 March 2005
Available online 4 May 2005

Abstract

Titanium dioxide is known to photodegrade organic contaminants in water and air with very low preference that often relies on the native ability of the contaminants to physisorb on the photocatalyst's surface. An approach for obtaining preferential photodegradation of diisopropyl methylphosphonate (DIMP), a chemical warfare agent simulant, is presented hereby. This approach is based on the construction of molecular recognition sites anchored on inert domains in the vicinity of photoactive sites. These sites are designed to chemisorb the target molecules and to "shuttle" them to the photocatalytic sites, where they are degraded. An increase in the photodegradation of DIMP by a factor greater than 4 is reported hereby, using Cu^{2+}, attached to a monolayer of 1,1-mercaptoundecanate (MUA) on gold, as the molecular recognition site. These sites retain their benevolent effect following washing with water, and, to a large extent, also under conditions where part of the organic functional groups of the MUA are destroyed.

Keywords: Photocatalysis; Titanium dioxide; Diisopropyl methylphosphonate; Surface-diffusion; "Adsorb & Shuttle"

1. Introduction

Decomposition of nerve agents is an issue of great interest, whether it is for neutralization of old chemical warfare materials, or chemical treatment of polluted areas. Among the various nerve agents is Sarin (isopropyl methylfluorophosphonate), which is often simulated by diisopropyl methylphosphonate (DIMP) [1,2]. There are several methods proposed for the decomposition of Sarin, such as biodegradation [3], combustion [4], pyrolysis [5], catalysis [6,7] and photocatalysis [8–10]. Photocatalysis seems to have a number of advantages over the other techniques, because of its low working temperature, low cost of photocatalyst (TiO_2) and possible usage of solar energy. That way, one may think, for example, of painted houses or take-off runways that can handle low levels of highly toxic gases.

For most cases, photocatalysis is based on the strong oxidation potential of OH radicals, which hardly differentiate between the type of target molecules [11]. This lack of sensitivity to the type of contaminants seems to be benevolent at first glance. However, it also implies that the photocatalyst does not differentiate between highly hazardous contaminants and organic contaminants of low toxicity. This shortcoming is farther aggravated by the fact that while many low-toxicity contaminants can be degraded by biological means, many of the highly hazardous materials are non-biodegradable. Thus expensive photons might be consumed for the degradation of less hazardous contaminants, including non-toxic by-products or intermediates.

Some selectivity in photocatalytic processes can be achieved by manipulating the adsorption of the contaminants on the photocatalyst surface, for example by controlling the surface's electric charge [12,13], by modifying the surface of TiO_2 particles with specific chelating agents [14], or by imprinting the target molecule into the TiO_2 particle [15,16].

Adsorption of contaminants in the vicinity of photocatalytic sites may increase photoefficiency. Here, the basic concept is based upon the physisorption of reactants on inert substrates, followed by their surface-diffusion to the

* Corresponding author. Tel.: +972 4 8292486; fax: +972 4 829 5672.
E-mail address: paz@tx.technion.ac.il (Y. Paz).

1010-6030/$ – see front matter © 2005 Elsevier B.V. All rights reserved.
doi:10.1016/j.jphotochem.2005.03.021

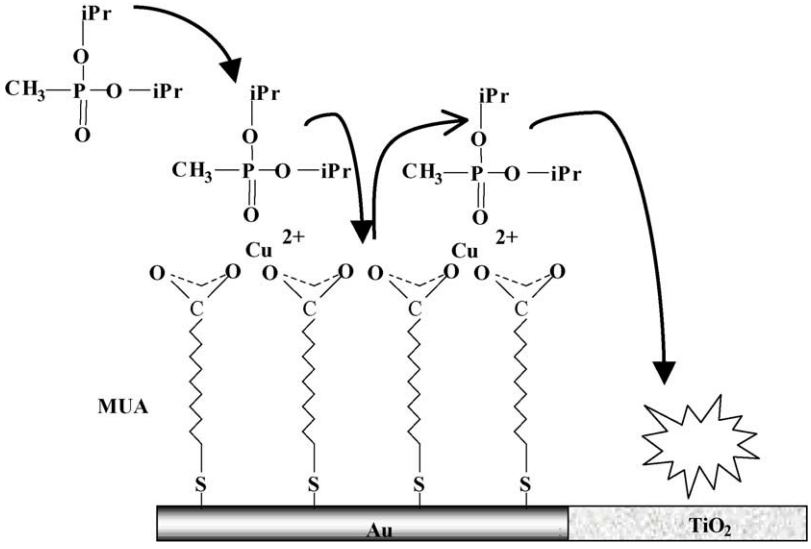

Fig. 1. The "Adsorb & Shuttle" concept.

interface between the adsorptive sites and the photocatalytic sites [17]. Although the adsorptive approach presented above helps in promoting the photodegradation of contaminants that normally do not adsorb on the photocatalyst surface, it cannot provide a comprehensive solution to the selectivity problem, since the adsorption selectivity of the inert domains is very poor and cannot be controlled.

A different, novel approach for obtaining high selectivity was proposed by our group recently, for the degradation of 2-methylnaphthoquinone [18,19]. The core of this Adsorb & Shuttle (A&S) approach is the construction of robust, immobilized organic molecular recognition sites (MRS) on inert domains, located on, or in the vicinity of, the photocatalyst. These molecular recognition sites are supposed to physisorb selectively the target molecules. Then, the adsorbed molecules surface-diffuse from site to site towards the interface between the inert domains and the photocatalytic domains, where they are destroyed (Fig. 1).

Recently, it was reported that DIMP adsorbs reversibly on a self-assembled monolayer of 1,1-mercaptoundecanoic acid (MUA), whose proton was substituted by Cu^{2+} (MUACu) [20,21]. To some extent, this report is related to early works, which showed that Cu^{2+} easily forms complexes with fluorophosphates [22]. Here, we present a first report on the preferential photodegradation of DIMP by means of "Adsorb & Shuttle", using MUACu as a molecular recognition site. Enhancement of the photocatalytic degradation of DIMP by a factor, as large as 6, is reported hereby. Since the affinity between MUACu and DIMP relies on the phosphonate group, which is common to DIMP and Sarin, it is expected that this system will be suitable also for Sarin.

2. Experimental

The model system in this study consisted of 1 in. silicon wafers substrates, coated with thin (100 nm), well-adhered layers of nano-crystalline TiO_2. The TiO_2 film was prepared by spin-coat application of an organotitante precursor made by chelating titanium tetraisopropoxide with acetylacetone, as was used before in the preparation of self-cleaning glass [23]. Thin films of gold were then deposited by evaporation, and patterned by a "lift-off" process into equal, 5 μm width, parallel stripes (Fig. 2) [19]. Once prepared, the substrates were coated by a monolayer of MUACu by a procedure consisting of cleaning in a commercial UV-Ozone cleaner (UVO 42–220, Jelight Ltd.) for 10 min, immersion in a 1 mM MUA/EtOH solution for 10 h, rinsing by EtOH and water and

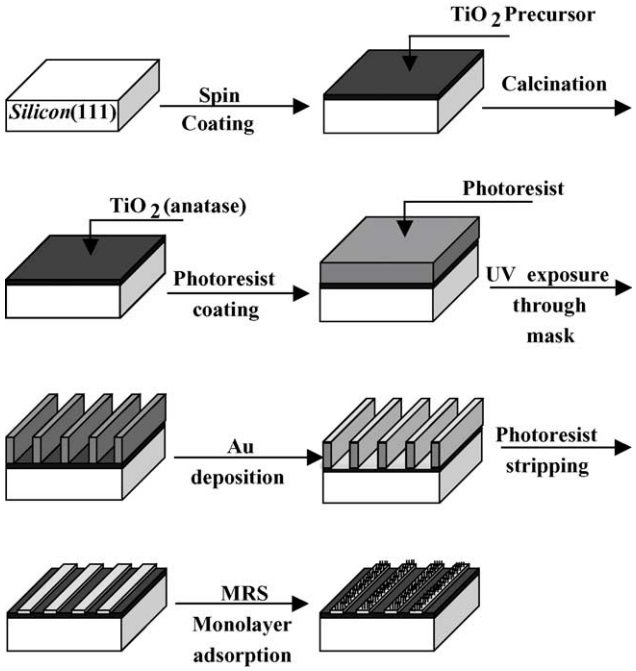

Fig. 2. The preparation of the samples.

immersing in a 2 mM $Cu(ClO_4)_2 \cdot 6H_2O$/EtOH solution for 10 min.

All patterned structures were characterized routinely during the preparation process by optical microscopy (Olympus BX60), to assure the good quality of the pattern-transfer process. The width of the titanium dioxide domains and that of the silicon domains were measured at the end of the process by a Vickers Instrument M41 measuring system. The depth of the stripes was measured by profilometry (alpha-step 500, Tencor Inc.) at the end of the process, to measure the corrugation of each of the domain types. Samples covered with self-assembled monolayers were characterized by Fourier transformed infra-red spectroscopy (Bruker IFS55, measured with 4 cm^{-1} resolution), in the reflection mode, as well as by Auger spectroscopy (Thermo VG Scientific Microlab 350 Scanning Auger Microscope) and XPS (Thermo VG Scientific Sigma Probe).

Photodegradation measurements were done in a closed cylinder vessel made of glass (40 ml), containing two 1.5 in. KBr windows. In each measurement three patterned 1 in. wafers were used, either with or without MUACu coating. Once closed, 0.001 ml of DIMP was injected into the cell through a septum. Evaporation and adsorption kinetics were then constantly monitored until steady state was reached. Then, the cell was illuminated by a low intensity (365 nm, 0.2 mW/cm^2 at the film surface) UV light, and its IR spectra was taken periodically.

3. Results and discussion

Fig. 3 presents the XPS spectra of the MRS samples prior to and following immersion in the $Cu(ClO_4)_2 \cdot 6H_2O$/EtOH solution. The replacement of MUA protons with the copper ions can be inferred from three major changes in the spectrum: the appearance of Cu^{2+} peak at a binding energy of 933.7 eV (A), the shift in the carbon 1S satellite typical for CO at a binding energy of 288.3 eV (C) and the shift of the oxygen 1S peak towards lower binding energies (B). This shift is the outcome of the deprotonation of the COOH that creates a negative ion where the electron binding is weaker.

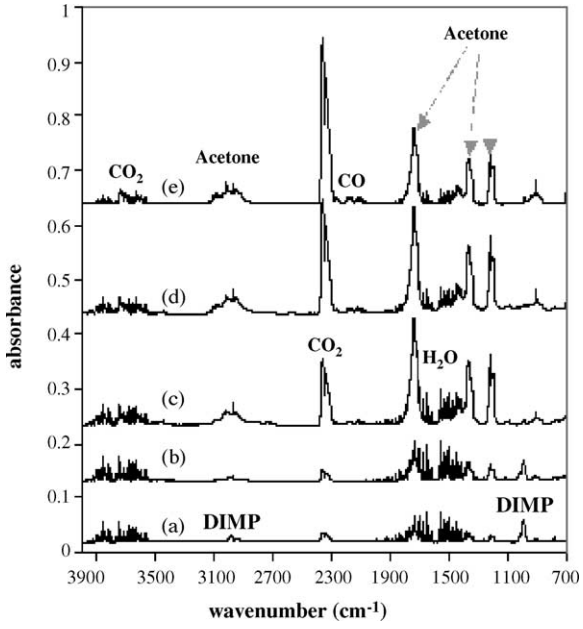

Fig. 4. The evolution of an FT-IR spectrum upon photodegradation of DIMP on TiO_2/MUACu: (a) before UV exposure, (b)–(e) following UV exposure for 3, 19, 39, 60 h, respectively.

Since DIMP is volatile, it is quite difficult to get direct evidence for enhanced adsorption of DIMP on the MUACu surface. Indirect evidence can be obtained by following the changes in the IR absorption of gas phase DIMP in the dark, right after introducing it into the reactor vessel. Indeed, such monitoring revealed faster adsorption kinetics (app. 1.5–2 times faster) with MUACu-containing samples, relative to patterned samples without MUACu. This difference is quite remarkable, taken that the area of the walls of the reactor was larger by more than one order of magnitude than the area covered with MUACu.

Fig. 4 presents the evolution of the spectra during a typical photocatalytic experiment, taken with MRS-coated patterned substrates. Typical DIMP peaks are observed at

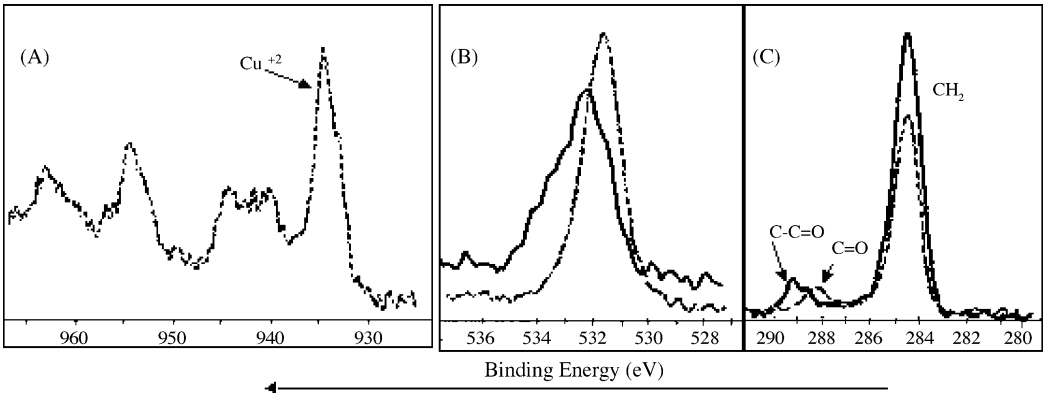

Fig. 3. XPS spectra of a MUA monolayer on a gold surface, prior to (solid line) and following (dashed line) immersion in the $Cu(ClO_4)_2 \cdot 6H_2O$/EtOH solution. (A) Copper 2p peak, (B) oxygen 1s peak, (C) carbon 1s peak.

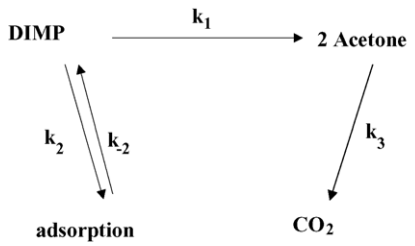

Fig. 5. The photodegradation scheme of DIMP.

917, 990, 1108, 1263 and 2982 cm^{-1}. The evolution of the spectrum upon photodegradation is clearly demonstrated in traces b, c, d and e. These changes correlate well with the degradation of DIMP, the formation of acetone (ν(CO) at 1735 cm^{-1}, δ(CH) at 1367 cm^{-1}, ν_a(CC) at 1212 cm^{-1}) as an intermediate product, and the formation of CO_2 (2348 cm^{-1}) and water as the final products. Some CO (2178, 2119 cm^{-1}) was noticed after 30 h of illumination, probably due to some lack of oxygen in the closed vessel. In addition, another peak at 912.2 cm^{-1}, which could be assigned to propanol, was observed. The evolution of the spectra during experiments with patterned substrates that had not been previously coated with MUACu revealed similar behavior qualitatively, except for the 912.2 cm^{-1} peak that was missing. Control experiments, done in the absence of TiO_2 substrates showed no evolution of the DIMP spectrum upon illumination, indicating that the degradation of DIMP was due to photocatalysis and not due to direct photochemistry. It is known that Cu^{2+} and some of its chelates may act as hydrolyzing catalysts for phosphonates [20]. It is noteworthy therefore, that exposure of DIMP to these two systems in the dark did not yield any significant amounts of acetone or CO_2, thus negating the possibility of such an effect.

Based on the evolution of the spectra it can be deduced that the photocatlytic degradation of DIMP proceeds as describes in Fig. 5, i.e. through the degradation of DIMP to the intermediate product acetone, later to be decomposed to CO_2 and water. This process occurs simultaneously with desorption of DIMP from the reactor's walls, which partially compensates for the loss of DIMP from the gas phase.

The effect of the MUACu MRS on the photodegradation of DIMP is demonstrated in Fig. 6, which shows the kinetics of formation of acetone for both types of substrates, based on the area of the acetone-related ν(CO) peak at 1735 cm^{-1}. The values in the figure were normalized according to the initial

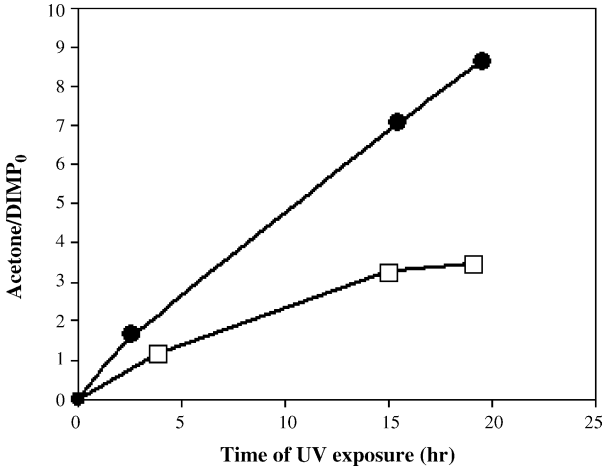

Fig. 6. The kinetics of acetone production during photodegradation of DIMP: (□) TiO_2/Au stripes (5 μm in width) without MRS; (●) TiO_2/Au stripes (5 μm in width) with MRS.

amount of DIMP as measured by FT-IR, to compensate for small (less than 10%) deviation in the initial concentration of DIMP. As depicted in the figure, at short exposure times, the rate of production of acetone in the presence of MUACu domains is by a factor of 3 higher than that observed with samples containing the same photocatalytic surface area but without MUACu. Similarly, examination of the production of CO_2 in these two systems revealed a faster increase in the mineralization rate for the MUACu-containing system, albeit by a factor of less than 3.

In order to find out whether the described-above enhancement in the amount of the intermediate product acetone by the MRS-containing system was due to enhanced DIMP degradation by the MUACu or due to slower photodegradation of acetone, the photodegradation of acetone was measured with various substrates. These substrates included structures made of stripes of TiO_2 (5 μm in width) and gold (5 μm in width), structures made of stripes of TiO_2 (5 μm in width) and gold (5 μm in width) coated with MUACu and thin films of titanium dioxide without any metal stripes. Care was taken to have the same active area in all three systems. Plotting the integrated absorbance (which is proportional to concentration) of the acetone peaks versus time yielded an exponential decaying curve ($R^2 > 0.99$), suggesting apparent first-order kinetics. Table 1 summarizes the degradation rate constants with these systems. For comparison, a first-order reaction rate constant, deduced from the acetone degradation

Table 1
The kinetic rate constants of the degradation of acetone with various substrates

Type of reactant	Type of substrate	Initial integrated absorbance of acetone (1735 cm^{-1})	The kinetic rate constants of the acetone degradation (h^{-1})
Acetone	TiO_2	26.4	0.012 ± 0.001
Acetone	TiO_2/Au	35.8	0.013 ± 0.001
Acetone	TiO_2/Au + MUA/Cu^{2+}	48.0	0.012 ± 0.001
Acetone, during photodegradation measurements of DIMP	TiO_2/Au + MUA/Cu^{2+}	18.4	0.014 ± 0.001

kinetics measured during the photodegradation of DIMP but at very long exposure times (i.e. once all DIMP was consumed) is also given.

As reflected in the table, the rate constants of these three systems were found to be identical ($0.012 \pm 0.001\,h^{-1}$), demonstrating that the presence of MUACu or gold do not have any effect (neither positive nor negative) on the photodegradation rate of acetone. Moreover, the kinetic rate constant of the photodegradation of acetone that was produced from DIMP was similar ($0.014\,h^{-1}$).

In order to quantify the benevolent effect of the "Adsorb & Shuttle" approach it is essential to calculate the extent by which the photodegradation rate of DIMP is improved by this approach. Taken that the contaminant is adsorbed reversibly on the reactor's walls, whose exposed area is approximately 25 times larger than that of the photocatalytic area, it is sensible to assume that a calculation based solely on changes in the IR signal of one of the DIMP peaks in the gas phase might be inaccurate.

The complex degradation reaction depicted in Fig. 5 can be described by two equations:

$$\frac{d[DIMP]}{dt} = \frac{A}{V}k_{-2}[DIMP]_{ADS} - k_2[DIMP] - k_1[DIMP] \quad (1)$$

$$\frac{d[acetone]}{dt} = k_1[DIMP] - k_3[acetone] \quad (2)$$

$$\frac{d[DIMP]_{ADS}}{dt} = \frac{V}{A}k_2[DIMP] - k_{-2}[DIMP]_{ADS} \quad (3)$$

$$[acetone]_{t=0} = 0, \qquad [DIMP]_{t=0} = [DIMP]_0 \quad (4)$$

Here V and A are the volume and the area of the reactor, respectively, $[DIMP]_{ADS}$ is the surface concentration of DIMP on the reactor's walls. k_1 and k_3 are volume-based reaction rate constants, hence reflect both reaction and mass transport, and accordingly should be considered as reactor dependent. In that manner, any surface diffusion effect in the "Adsorb & Shuttle" is lumped into k_1.

Adsorption measurements of DIMP in the absence of light revealed that under the conditions used in the above-mentioned photodegradation experiments, the number of molecules adsorbed on the various surfaces of the reactor is approximately 12 times larger than what was left in the gas phase. Taken that in our experiments the photodegradation began only after the process of adsorption reached its steady state, and that, by virtue of the low photon flux that was used, the photodegradation time scales were larger than the adsorption time scale, it is reasonable to assume a pseudo-steady-state with respect to $[DIMP]_{ADS}$. Under this assumption, it is possible to calculate the ratio between k_1 in a system containing the MRS and k_1 in the control system. This ratio can be calculated either based on the IR kinetics of any of the DIMP peaks, or based on the rise and fall of the acetone peaks. Calculating k_1 on the basis of the disappearance of the DIMP signals disregards the contribution from the reactor's walls, hence gives an upper bound to the true k_1. Doing so, assuming first-order kinetics gives k_1 values of $0.16\,h^{-1}$ and $0.04\,h^{-1}$, reflecting an improvement of the reaction rate constant by a factor of 4, due to the presence of the molecular recognition sites.

Based on the above-mentioned assumptions, Eq. (2) can be solved analytically:

$$[acetone] = \frac{[DIMP]_0 k_1}{k_3 - k_1}[e^{-k_1 t} - e^{-k_3 t}] \quad (5)$$

By differentiating this expression, the time where the concentration of acetone is maximal can be calculated as:

$$t_{max} = \frac{\ln[k_3/k_1]}{k_3 - k_1} \quad (6)$$

Substituting (6) into (5) gives the maximal acetone concentration:

$$[acetone]_{max} = [DIMP]_0 \left[\frac{k_3}{k_1}\right]^{-k_3/(k_3-k_1)} \quad (7)$$

From which it is possible to relate the amount of acetone at each time, relative to its maximal amount, with the value of k_1:

$$\frac{[acetone]}{[acetone]_{max}} = \frac{k_1}{k_3 - k_1}\left[\frac{k_3}{k_1}\right]^{k_3/(k_3-k_1)}[e^{-k_1 t} - e^{-k_3 t}] \quad (8)$$

This expression provides a way to calculate k_1 from the variations in the IR peaks of acetone as a function of time. Taking the previously calculated value of k_3 ($0.012\,h^{-1}$), it is possible to fit the kinetics of acetone formation and disappearance using a single adjustable parameter (k_1). Such a fitting is presented in Fig. 7. According to the fitting, k_1 was found to be $0.1\,h^{-1}$ for the MRS structure, and $0.01\,h^{-1}$ for the non-MRS structure, reflecting an increase by a factor of 10 in the value of k_1.

Hence, it can be concluded that the value of k_1 was improved, under the above-mentioned experimental conditions,

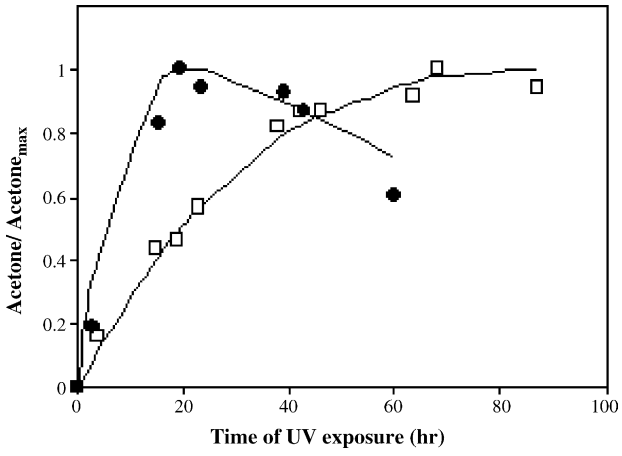

Fig. 7. The kinetics of acetone production during photodegradation of DIMP and their fit according to Eq. (8): (□) TiO_2/Au stripes (5 μm in width) without MRS; (●) TiO_2/Au stripes (5 μm in width) with MRS.

approximately by a factor of 4–10. The difference in the two enhancement values calculated by the two methods can be attributed to some deviation from the pseudo-steady-state condition assumed for the adsorbed DIMP, as well as from possible contribution by direct mineralization.

Since the molecular recognition sites are organic, care should be taken to prevent their destruction by the oxidizing species formed on the titanium dioxide surface. Obviously, this means that the MRS should not be constructed directly on the photocatalytic titanium dioxide surface, as indeed is the case here. Moreover, it is needed to assure that MRS located on inert sites, adjacent to photocatalytic domains, are not prone to an attack by oxidizing species, diffusing from the photocatalyst domains to the inert domains, as may happen when the inert domains are made of silicon dioxide [24]. In this context, it is noteworthy that a previous work showed that-self assembled monolayers chemisorbed on metallic domains in the vicinity of titanium dioxide are stable towards remote degradation [19,25]. More study is underway.

Auger spectra of a MUACu-containing gold stripes, prior to, and following, 60 h of illumination revealed a noticeable decrease in the carbon signal relative to that of the sulfur, indicating that at least part of the hydrocarbon backbone of the MRS was degraded upon illumination. This photoinduced degradation of the MRS may explain why propanol was observed in the gas phase spectra of DIMP that was photodegraded using TiO_2/MUACu substrates, but not in the spectra of DIMP that was photodegraded using TiO_2 substrates. The source of this degradation of the MRS, that had not been observed before with MRS made of thiolated β-cyclodextrin nor with thiolated alkyl chains is probably connected with the larger UV dosage used in the MUACu experiments, in comparison with the thiolated β-cyclodextrin experiments. The possibility that this effect is connected to the presence of Cu^{2+} was negated, since repeating these experiments with a monolayer of MUA whose proton had not been replaced with copper also revealed some degradation of the carbon chain attached to the inert gold.

That the MRS is being changed upon UV illumination can be observed also by analyzing the XPS peaks of copper (Fig. 8), at a binding energy of 935 eV. Here, a doublet that could be assigned to a mixture of oxidating states existing prior to illumination was shifted following 60 h of UV illumination into lower binding energy (932 eV). Based on the binding energy, it is impossible to clarify, whether the post-illumination peak reflects Cu^0 or Cu^{1+}. However, by plotting the Wagner Plot it could be deduced that it is most likely that the reduced copper specie was Cu^{1+} and not Cu^0. In principle, the reduction of the copper ion following illumination could be deleterious for its mass transport effect on DIMP. Fortunately, the copper tends to re-oxidize itself in air to Cu^{2+} (Fig. 8, trace C), such that it should be able to recover itself in humid air.

In order to study the feasibility of this concept in real systems, two successive experiments were performed, and their results were compared. Fig. 9 presents the ratio between

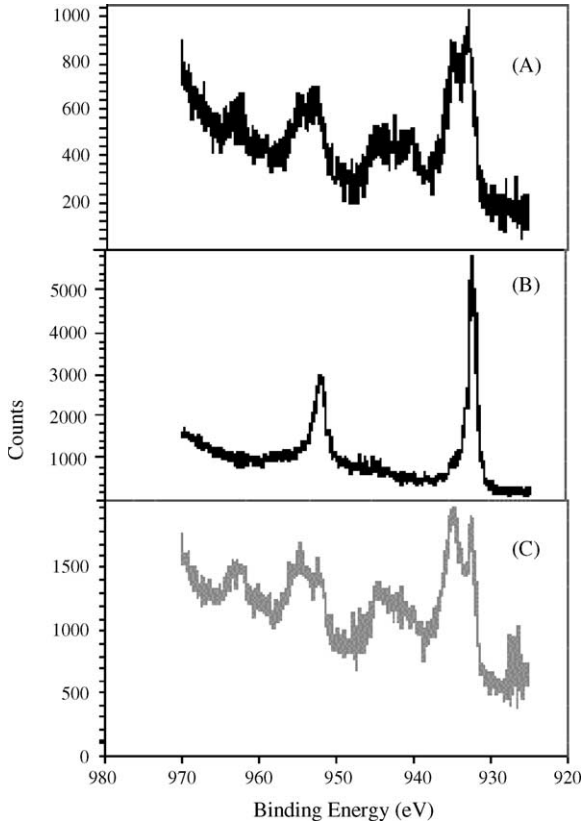

Fig. 8. The XPS spectra of the copper ion on a MUACu patterned structure: (A) before UV exposure, (B) after 60 h of UV exposure, (C) after 60 h of UV exposure, followed by exposure to air for several hours.

acetone concentration at a given time and its maximal value, for a system that contained MUACu inert domains (A) and for a system that did not contain such structures (B). As demonstrated in the figure, the maximal values of acetone were obtained after 45 and 70 h of illumination for the first and the second run, respectively. This increase in the time reflects some deterioration in the benevolent effect of the patterned structure. Yet, even at this situation, its performance was by far better than the performance of a non-patterned substrate, where the time required to get maximal acetone concentration under the same conditions was approximately 130 h (Fig. 9(B)). As mentioned before (Fig. 8), the copper seems to remain on the surface in an oxidized form, even when part of the alkyl chain of the MRS is consumed. XPS measurements performed on the patterned structures prior to and following exposure to UV revealed a slight shift in the sulfur $2P_{3/2}$ binding energy from 163 to 162.7 eV. According to the literature [26], these binding energies correspond to that of reduced sulfur; the binding energy of sulfides being slightly lower than that of mercaptans. Hence, one may propose that in cases where the alkyl chain was consumed, the positive copper ion can still be attached to the surface, through an interaction with chemisorbed sulfur, thus retaining its effectiveness for the photodegradation of DIMP.

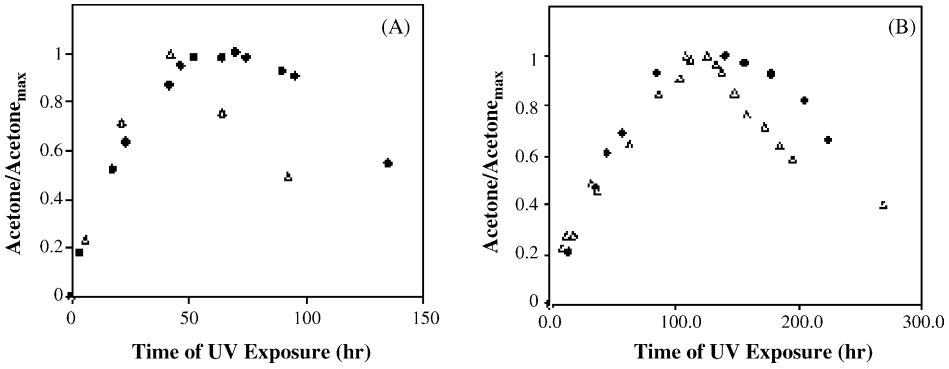

Fig. 9. The ratio between acetone concentration at a given time and its maximum value during DIMP photodegradation on (A) (Δ) fresh TiO_2/Au+MUACu; (●) reused TiO_2/Au+MUACu; (B) (Δ) fresh TiO_2; (●) reused TiO_2.

The possible effect of washing with water on the performance of MUACu-loaded structures is very important for the developing of outdoor photocatalytic paint. The subject was studied by washing thoroughly the samples with water prior to performing the photocatalytic tests and comparing the degradation kinetics. No adverse effect of washing was recorded with the patterned MUACu samples, regardless whether the measurements were performed with "as produced" samples, or with samples that had been tested for the second time. The absence of any washing effect in the second run seems to support our claim that the copper remained attached to the surface. In accordance, analyzing the surface following the thorough washing revealed only a minute effect on the surface concentration of copper.

Since the benevolent effect of MUACu stems from the specific interaction between the copper ions and the DIMP molecules, it was decided to evaluate the feasibility of using copper ions deposited directly on the titanium dioxide surface. For that, non-patterned TiO_2 films were immersed in a $Cu(ClO_4)_2{\cdot}H_2O$/EtOH solution for 10 min. Photocatalytic measurements revealed an enhancement in the production of acetone that was comparable with that of the patterned wafers. AES measurements done post experiment on the non-patterned wafers that had been previously immersed in the copper solution revealed high concentration of phosphorous on the titanium dioxide surface, and absence of copper, in contrast to the case of MUACu where the copper could be noticed on the inert domains at the end of the process. This absence of copper on the surface of the non-patterned samples can be explained by the formation of a relatively thick layer of the phosphorous residue.

The same washing effect experiments done with the patterned samples were performed also with the copper-immersed samples. Here, washing reduced significantly the enhancement (almost doubled the rise time of acetone production). In parallel, XPS measurements indicated the removal of approximately 75% of the copper ions from the surface upon washing with water, pointing out the need for well-adhered copper ions in order to promote the photodegradation of phospho-organic compounds. Such adherence can be obtained through a carboxylate group or even a sulfide as discussed above.

4. Conclusion

A new system, demonstrating the "Adsorb & Shuttle" approach, was presented in this manuscript. This system utilizes the affinity between 1,1-mercaptoundecanoic acid (MUA) whose proton was substituted by Cu^{2+} and diisopropyl methylphosphonate (DIMP), a chemical warfare agent simulant. An improvement by a factor of app. 6 was obtained, for a structure, made of alternating stripes of titanium dioxide and molecular recognition sites on gold, both having 5 μm in width. It is sensible to believe that much greater improvement is possible in powders, where the average diffusion length is much smaller than the 1.3 μm that is in the present experiments.

The fact that the benevolent effect of the MUACu was noticed with DIMP, but not with acetone, evidently shows that the "Adsorb & Shuttle" approach may serve not only to increase degradation rates but also to induce photodegradation in a preferential manner. Such preferential activity is of great importance in particular in systems where the intermediate products are far less hazardous than the initial reactants, as indeed happens in this system, and may also happen in the photodegradation of many chemical warfare agents.

The results presented in this work point also to the need for better protection of the molecular recognition sites from photodegradation. Alternatively, they also suggest a way to detour this problem, based on the adherence between the copper ions and the residues of the MUA photodegradation, most likely the sulfides. A continuation of this research along these lines is underway.

Acknowledgements

This work was funded by the Israel Science Foundation under contract number 53/02. The assistance of Dr. Reuven Brenner in performing the AES and XPS measurements is also acknowledged.

References

[1] O.P. Korobeinichev, A.A. Chernov, T.A. Bolshova, Combust. Flame 123 (2000) 412.
[2] M.V. Buchanan, R.L. Hettich, J.H. Xu, L.C. Waters, A. Watson, J. Hazard. Mater. 42 (1995) 49.
[3] Y. Zhang, R.L. Autenrieth, J.S. Bonner, S.P. Harvey, J.R. Wild, Biotechnol. Bioeng. 64 (1999) 221.
[4] O.P. Korobeinichev, A.A. Chernov, T.A. Bolshova, Combust. Flame 123 (2000) 412.
[5] E.J.P. Zegers, E.M. Fisher, Combust. Flame 115 (1998) 230.
[6] R.W. Baier, S.W. Weller, Ind. Eng. Chem. Process Des. Dev. 6 (1967) 380.
[7] N.C. Blacker, P.H. Findlay, D.C. Sherrington, Polym. Adv. Technol. 12 (2001) 183.
[8] K.E. O'Shea, S. Beightol, I. Garcia, M. Agular, D.V. Kalen, W.J. Cooper, J. Photochem. Photobiol. A: Chem. 107 (1997) 221.
[9] T.N. Obee, S. Satyapal, J. Photochem. Photobiol. A: Chem. 118 (1998) 45.
[10] C.N. Rusu, J.T. Yates, J. Phys. Chem. B 104 (2000) 12299.
[11] R.W. Matthews, Water Res. 20 (1986) 569.
[12] M.A. Fox, M.T. Dulay, Chem. Rev. 93 (1993) 341.
[13] P. Salvador, J. Electrochem. Soc. 128 (1981) 1895.
[14] R.J. Kriek, W.J. Engelbrecht, J.J. Cruywagen, J. S. Afr. Inst. Mining Metall. 95 (1995) 75.
[15] (a) M. Zayats, M. Lahav, A.B. Kharitonov, I. Willner, Tetrahedron 58 (2002) 815;
(b) M. Lahav, A.B. Kharitonov, O. Katz, I. Willner, Anal. Chem. 73 (2001) 720.
[16] (a) S.-W. Lee, I. Ichinose, T. Kunitake, Langmuir 14 (1998) 2857;
(b) S.-W. Lee, I. Ichinose, T. Kunitake, Chem. Lett. 1193 (1998);
(c) Y. Lvov, K. Ariga, I. Ichinose, T. Kunitake, J. Am. Chem. Soc. 117 (1995) 6117.
[17] (a) G. Dagan, S. Sampath, O. Lev, Chem. Mater. 7 (1995) 446;
(b) H. Hidaka, K. Nohara, J. Zhao, N. Serpone, E. Pelizzetti, J. Photochem. Photobiol. A: Chem. 64 (1992) 247;
(c) S. Sampath, H. Uchida, H. Yoneyama, J. Catal. 149 (1994) 189.
[18] S. Ghosh-Mukerji, M. Schvartzman, H. Haick, Y. Paz, J. Am. Chem. Soc. 123 (2001) 10776.
[19] S. Ghosh-Mukerji, H. Haick, Y. Paz, J. Photochem. Photobiol. A 160 (2003) 77.
[20] L.J. Kepley, R.M. Crooks, Anal. Chem. 64 (1992) 3191.
[21] P.G. Datskos, M.J. Sepaniak, C.A. Tipple, N. Lavrik, Sens. Actuators B 76 (2001) 393.
[22] T. Wagner-Jauregg, B.E. Hackley, T.A. Lies, O.O. Owens, R. Proper, J. Am. Chem. Soc. 77 (1955) 922.
[23] Y. Paz, Z. Luo, L. Rabenberg, A. Heller, J. Mater. Res. 10 (1995) 2842.
[24] H. Haick, Y. Paz, J. Phys. Chem. B 105 (2001) 3045.
[25] E. Zemel, H. Haick, Y. Paz, J. Adv. Oxid. Technol. 5 (2002) 27.
[26] C.D. Wagner, Handbook of X-Ray Photoelectron Spectroscopy, Perkin-Elmer Corporation, Minnesota, 1979.